Rydberg Excitons in the Presence of an Ultralow-Density Electron-Hole Plasma

J. Heckötter,[1] M. Freitag,[1] D. Fröhlich,[1] M. Aßmann,[1] M. Bayer,[1] P. Grünwald,[2] F. Schöne,[2]
D. Semkat,[3] H. Stolz,[2] and S. Scheel[2]

[1]*Experimentelle Physik 2, Technische Universität Dortmund, D-44221 Dortmund, Germany*
[2]*Institut für Physik, Universität Rostock, Albert-Einstein-Straße 23-24, D-18059 Rostock, Germany*
[3]*Institut für Physik, Ernst-Moritz-Arndt-Universität Greifswald, Felix-Hausdorff-Straße 6, D-17489 Greifswald, Germany*

We study the Rydberg exciton absorption of Cu_2O in the presence of free carriers injected by above-band-gap illumination. Already at plasma densities ρ_{EH} below one hundredth electron-hole pair per μm^3, exciton lines are bleached, starting from the highest observed principal quantum number, while their energies remain constant. Simultaneously, the band gap decreases by correlation effects with the plasma. An exciton line loses oscillator strength when the band gap approaches its energy, vanishing completely at the crossing point. Adapting a plasma-physics description, we describe the observations by an effective Bohr radius that increases with rising plasma density, reflecting the Coulomb interaction screening by the plasma.

Introduction.—Coulomb-correlated two-particle complexes in the presence of free charges represent a central problem of many-body phenomena in physics. In semiconductors, corresponding studies were performed for excitons, bound complexes of a negatively charged electron, and a positively charged hole. When increasing the exciton density a smooth transition is expected from an excitonic insulator to an electron-hole plasma with an extended coexistence phase in between [1–3]. This transition, so far assessed for the ground state exciton only, occurs around the Mott density [4,5], at which the intercarrier separation is comparable to the exciton Bohr radius. The Mott transition was studied by photoluminescence spectroscopy, providing limited information: hardly any changes of the exciton emission are observed up to densities close to the Mott density. Only then an energy shift combined with a line broadening may be identified, while the change of band gap to electron-hole transitions could not be measured [3]. The line shift, if resolvable at all, remained weak with the meV resolution achieved so far, which was attributed to an approximate compensation of correlation and screening effects. Insight into quantities such as band gap renormalization, chemical potentials, etc., required a line shape analysis based on theoretical models.

Here, we study the excitons of the yellow series in cuprous oxide in highly excited states [6]. The absorption of these Rydberg excitons is measured in the presence of free carriers injected above the band gap at densities orders of magnitude below the ground state exciton Mott density. Simultaneously, we monitor the change of the band gap. Already at electron-hole (EH) plasma densities of $\rho_{EH} = 0.01\ \mu m^{-3}$, we find a band gap reduction comparable to the binding energies of the high lying excitons whose energies, on the other hand, do not shift at all. When

the band gap approaches an exciton, it loses oscillator strength and vanishes completely when the gap crosses its energy so that it becomes located in the continuum: this crossing could, to the best of our knowledge, not be resolved before. The plasma density required for ionizing an exciton scales with its principal quantum number as n^{-4}, providing systematic insight into the Mott transition.

Experiment.—In experiment, a Cu_2O crystal of 30 μm thickness is placed in a liquid helium cryostat. For excitation we use two frequency-stabilized dye lasers. The photon energy of the probe laser is used to scan the exciton spectrum, while the pump laser injects electron-hole pairs at an energy above the band gap of Cu_2O. The pump spot size of 0.3 mm is slightly larger than the probe spot to ensure homogeneous excitation. After transmission through the sample, the probe laser light is detected by a photodiode.

Figure 1 shows absorption spectra of Rydberg excitons ($T = 1.35$ K), from $n = 10$ to above the band gap. Without pump, P excitons up to $n = 23$ are observed (top trace) [7]. The absorption lines appear on a smooth background which can be separated in two ranges. Above the gap, the spectrum is flat due to forbidden, direct electron-hole transitions into the continuum, adding up to a steplike increase of the absorption at the gap (dashed line) [8,9]. Thereby, we can assess the band gap energy E_{gap} by the point from which on the absorption is approximately constant, see arrows. Below the gap, the background spectrum is expected to be given by optical phonon-assisted absorption into the $1S$ yellow exciton and direct absorption into green excitons [10]. In the small energy range shown (1 meV only), this contribution would be almost constant (variation $< 1\%$). In contrast to these expectations for an "ideal" semiconductor, the absorption shows a smooth rise (see dashed line) which can be approximated by an
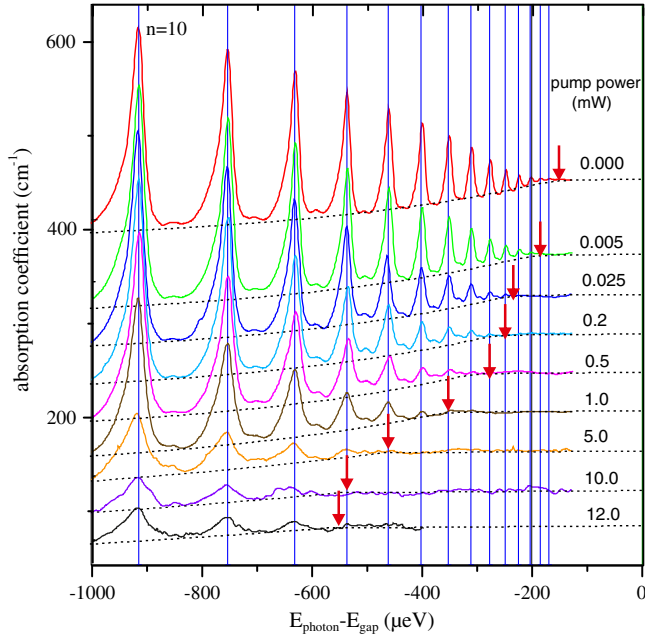
FIG. 1. Absorption spectra of Rydberg excitons from $n = 10$ onwards at $T = 1.35$ K under action of a pump laser with photon energy 2.2 eV, operated at different powers. Top trace shows absorption without pump. Dashed lines show absorption into continuum above the band gap, extended by an Urbach tail to lower energies. Arrows indicate the band gap. Traces are shifted vertically for clarity. Zero energy corresponds to $E_{gap} = 2.17208$ eV.

FIG. 2. (a) Comparison of experiment (open dots) and theory (red bars, scaling with $\rho_{EH}^{-0.25}$) for maximum observed exciton (left ordinate) vs pump laser power (bottom abscissa) and corresponding plasma density (top abscissa). Additionally, the dependence of the band gap shift (right ordinate) on these parameters is shown (full dots, experiment; blue line, theory following a $\rho_{EH}^{0.5}$ dependence). (b) Comparison of dependences of measured peak area [17] and relative oscillator strength, calculated from effective Bohr radius $a_{B\,eff}$ and effective quantum number n_{eff}, on band gap shift for $n = 15$ (red), $n = 17$ (blue), and $n = 19$ (magenta).

exponential function as for an Urbach tail [11]. We attribute this tail to the influence of residual charged impurities due to incomplete compensation in Cu_2O [12], leading to weak p-type doping and providing a disorder potential, by which the absorption is extended from the gap towards lower energies. Because of these charges, the transition to constant absorption also does not occur at the nominal band gap but is shifted to lower energies by about $\Delta_0 = 150$ μeV. The nominal band gap can be obtained by extrapolating the exciton energies (not affected by impurities, see below) in the hydrogenlike series, $E_{gap} - Ry/(n - \delta_P)^2$ with Rydberg energy $Ry = 86$ meV and P-exciton quantum defect $\delta_P = 0.32$, to $n \to \infty$, yielding $E_{gap} = 2.17208$ eV [13].

The other traces in Fig. 1 show the absorption with the pump switched on, at a fixed pump photon energy of 2.20 eV, about 28 meV above the band gap. The pump power is varied from 5 μW to 12 mW (power densities from 50 μW/mm^2 to 120 mW/mm^2). Already for the lowest powers, the exciton absorption decreases, as evidenced by the disappearance of resonances at the high energy flank. This is associated with a reduction of the apparent band gap position at the transition from Urbach tail to flat continuum (see arrows). More and more lines vanish with increasing pump power starting from the highest ones, until for the
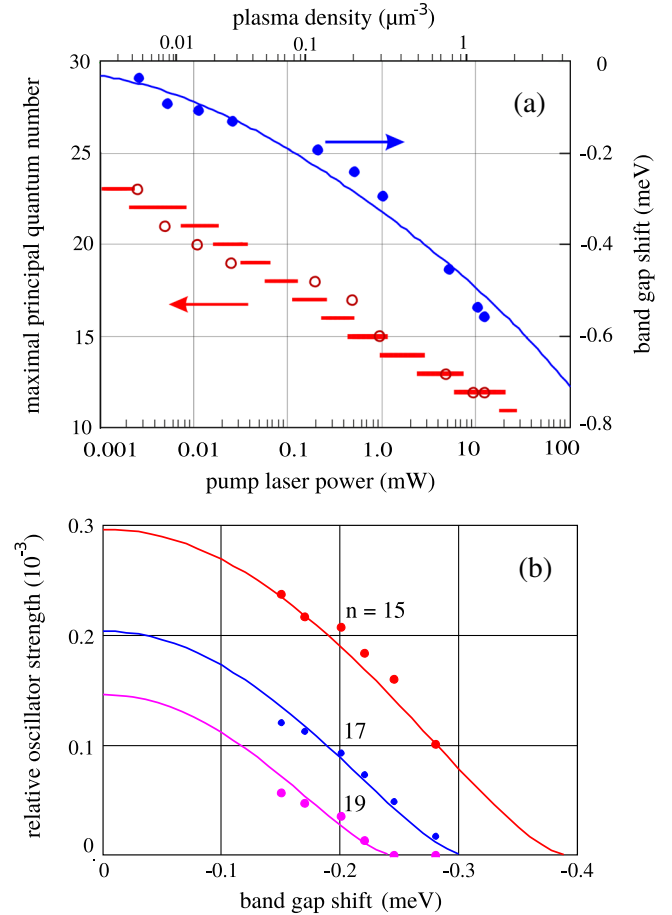
strongest pump only states up to $n = 12$ are observed. A state disappears when the band gap crosses its energy, which so far had not been observed directly due to broad exciton lines and unresolvable band gaps.

In Fig. 2 key experimental findings derived from these spectra are summarized: Panel (a) shows the variation of highest observed principal quantum number (open dots) and band gap shift (full dots) with pump power. Panel (b) gives the decrease of the $n = 15, 17, 19$ absorption line areas vs band gap shift. Along with these changes, the energies of the exciton lines remain constant with μeV accuracy. Further, within the range where it can be reasonably estimated, also the linewidths of the resonances do not change notably [14]. Therefore, the exciton disappearance cannot be related to scattering with the plasma

because the associated lifetime reduction would lead to resonance broadening. Rather, it must be related to a change of the exciton envelope functions by plasma dressing as known for atoms [15] but not considered yet for semiconductors. That the exciton coherence is not destroyed by the plasma is seen also from the weak absorption peaks between the P excitons, arising from exciting coherent superpositions of the two adjacent P excitons [16]. Dephasing by exciton-carrier scattering would prevent excitation of these superpositions which appear until the band gap hits the higher lying involved exciton.

Theory.—The free carriers induced by above-band-gap excitation cause self-energy corrections and lower the band gap akin to the Mott effect [15,18,19]. In Cu$_2$O, the plasma density [20] where the $1S$ exciton vanishes in the continuum, is $\rho_{Mott} \approx 3 \times 10^{18}$ cm^{-3}. Here, we are interested in the Mott-effect analogs for large n occurring at much lower plasma densities. Whether the electron-hole plasma is a degenerate Fermi gas, can be assessed by its degeneracy parameter given by the product of the cube of the thermal wavelength $\Lambda_{th} = \hbar\sqrt{2\pi/\mu_{EH}k_BT_{EH}}$ (μ_{EH}, reduced mass of electron and hole) times the plasma density, $\Lambda_{th}^3\rho_{EH}$ [15]. In the low-density regime as in our experiments, the degeneracy parameter is much smaller than unity. Here, even for large densities of $\rho_{EH} = 1$ μm^{-3} and plasma temperature of $T_{EH} = 5$ K, it is only about 0.15, so that the nondegenerate classical Debye theory [15] can be applied [21], where the correlation part of chemical potential Δ_D is a good measure for the band gap shift Δ and depends on plasma density and temperature through $\Delta_D = -\kappa e^2/(4\pi\epsilon_0\epsilon_b)$ with κ being the inverse screening length. For a plasma with two components differing in effective temperature, κ is given by $\kappa^2 = 2\rho_{EH}e^2/(\epsilon_0\epsilon_bk_BT_{sc})$ with the effective screening temperature $1/T_{sc} = (1/T_e + 1/T_h)/2$. T_e and T_h are the electron and hole temperatures, which in nonequilibrium differ from the crystal temperature T (see Supplemental Material [24]). As a consequence, $-\Delta_D \propto \sqrt{\rho_{EH}}$ for $T_{sc} = $ const.

We expect an exciton state to vanish when the chemical potential [see Fig. 3(a)] is large enough for the band gap to shift below this state. For the $n = 25$ exciton, the highest principal quantum number revealed so far in experiment [6], this happens for a density as low as $\rho_{EH} \approx 10^{-2}$ μm^{-3} for $T_{sc} = 1.35$ K. This low density corresponds to a screening length of 1.6 μm, where the statistical plasma influence entails a minute band gap renormalization, which we are nonetheless able to probe by determining the energy at which the smoothly increasing absorption on which the exciton lines are superimposed transforms characteristically into a basically flat absorption with no indications for exciton resonances. For a density about 2 orders of magnitude larger, but still 6 orders below the $1S$ Mott density, the $n = 10$ exciton would no longer be observable. At higher T_{sc}, the plasma degeneracy is reduced so that
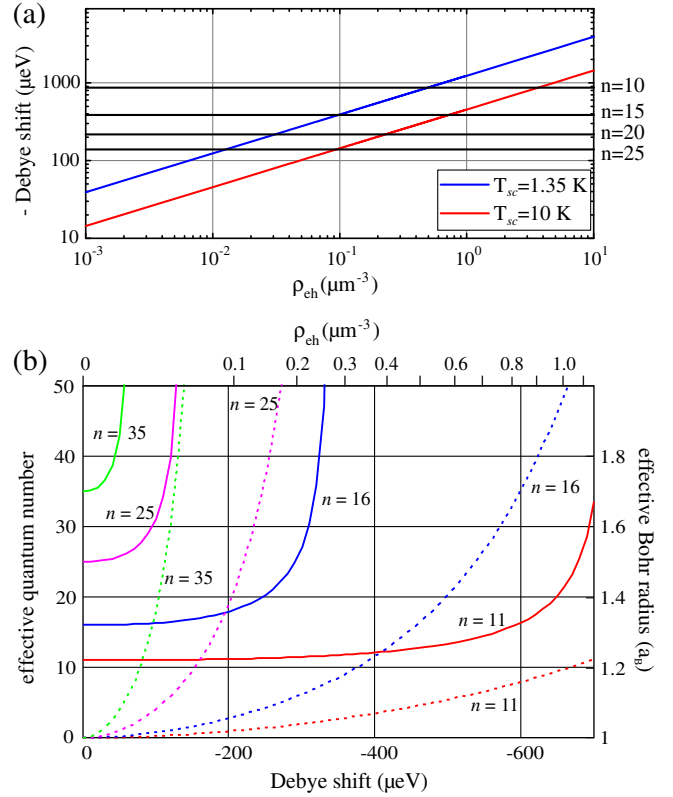

FIG. 3. (a) Debye shift Δ_D of band gap vs plasma density at $T_{sc} = 1.35$ K (blue line) and at $T_{sc} = 10$ K (red line), representing the limits of equilibrium and maximal out-of-equilibrium case in experiment (see Supplemental Material [24]). Horizontal lines give binding energies of $n = 25, 20, 15, 10$ excitons (from bottom to top). Crossing points give critical plasma densities for dissociation of state n. (b) Dependence of effective principal quantum number n_{eff} (full lines, left ordinate) and effective Bohr radius $a_{B\,eff}$ in units a_B (dashed lines, right ordinate) on Debye shift Δ_D for $n = 11, 16, 25, 35$. The upper abscissa shows corresponding ρ_{EH} at $T_{sc} = 5$ K.

higher densities are required for similar band gap reductions (compare $T_{sc} = 1.35$ and 10 K).

For relation with experiment, we have to connect the plasma density ρ_{EH} to the applied pump power. The density obeys, for low pump powers, the rate equation $d\rho_{EH}/dt = G - \Gamma_{EH}\rho_{EH} - \Gamma_{rc}\rho_{EH}^2$ with the generation rate G proportional to the pump power, the inverse lifetime Γ_{EH}, and the bimolecular recombination rate Γ_{rc}, while for high powers we have to solve the full set of rate equations (see Supplemental Material [24]). The involved relaxation rates Γ_{EH} and Γ_{rc} also determine the plasma temperature (the shorter the lifetime is, the hotter is the plasma) and thus the band gap shift [Fig. 2(a)]. To isolate the plasma influence, we have corrected the measured Δ by the band gap shift due to impurities, Δ_0: $\sqrt{\Delta^2 - \Delta_0^2}$. The density of uncompensated carriers due to impurities, estimated from Δ_0, is about 0.01 μm^{-3}.

With the appropriate plasma relaxation parameters ($1/\Gamma_{EH} = 18$ ns and $\Gamma_{rc} = 1.15 \times 10^{-12}$ cm^3/ns), we obtain

the blue line for Δ_D in Fig. 2(a) as a function of laser power and plasma density (bottom and top abscissa). The experimental data follow the expected dependence on $\rho_{EH}^{0.5}$, and confirm that extremely low plasma densities provide already a band gap renormalization larger than the binding energies of high lying Rydberg excitons so that they disappear in the continuum according to the Mott criterion ($\Delta_D = \mathrm{Ry}/n^2$, neglecting the quantum defect). Hence, we find for the critical plasma density $\rho_{EH,c}(n)$, at which the exciton n vanishes in the continuum, a scaling with n^{-4}. Vice versa, the maximum observable n scales with plasma density as $\rho_{EH}^{-0.25}$, in reasonable agreement with the observed trend. The reduction of the band gap is a first-order plasma process, while, for the exciton energies, various many-particle effects compensate each other largely, e.g., self-energy, Pauli blocking, and screening [15,22]. That the compensation is exact within micro-electron-volt accuracy, is still surprising and asks for more elaborate calculations.

Similarly striking is the decrease of oscillator strength of an exciton, starting well below the corresponding $\rho_{EH,c}(n)$ [see Fig. 2(b)]. For P excitons, the oscillator strength is determined by the squared slope of the wave function at zero electron-hole separation: $f_{\mathrm{osc}}(n) \propto [\partial\phi(r)/\partial r|_{r=0}]^2 = (n^2 - 1)/(3\pi a_B^5 n^5)$ with the exciton Bohr radius a_B [8]. Similar to atomic plasmas [15,29,30], the hydrogen wave function is changed according to a modified Wannier equation (i.e., the Schrödinger equation for the relative electron-hole motion) with a screened Coulomb potential that, in first approximation, can be taken as the Debye potential $V_D(r) = e^2/(4\pi\epsilon_0\epsilon_b r)\exp(-\kappa r)$ [15]. For low plasma densities as here one can use a variational adjustment of the Bohr radius to obtain the dressed hydrogen wave function [29]. This gives for the P-exciton energy in state n (with $x = a_{B\,\mathrm{eff}}/a_B$ and $\xi = \kappa a_B/2$):

$$\langle E_P(n)\rangle = \Delta_D + \frac{\mathrm{Ry}}{n^2}\left(\frac{1}{x^2} - \frac{2}{x}\frac{1}{(1 + n\xi x)^{2n}}\,{}_2F_1\right). \quad (1)$$

Here ${}_2F_1(-1 - n, 2 - n, 1, (n\xi x)^2)$ is the hypergeometric function. The effective Bohr radii $a_{B\,\mathrm{eff}} > a_B$ obtained in this way for different n are shown in Fig. 3(b). To account for the plasma insensitivity of exciton energies, we ascribe to each of them an effective quantum number n_{eff} such that $\langle E_P(n)\rangle$ remains equal to that of the unperturbed state, independent of the band edge shift Δ_D. The values of n_{eff} are also shown in Fig. 3(b) [31]. $a_{B\,\mathrm{eff}}$ increases, starting from a_B, already at relatively small band edge shifts and, hence, low plasma densities, corresponding to an effectively increased wave function extension due to screening. n_{eff} stays almost constant for low densities, but increases rapidly when the band gap approaches state n.

Assuming the same dependence on Bohr radius and principal quantum number for the perturbed states, but with $a_{B\,\mathrm{eff}}$ and n_{eff}, the oscillator strength and, therefore, the

peak area depend on density and temperature of the electron-hole plasma via the band edge shift. The resulting comparison of the relative oscillator strength $\{f_{\mathrm{rel}}(n) = (n_{\mathrm{eff}}^2 - 1)/[(a_{B\,\mathrm{eff}}/a_B)^5 n_{\mathrm{eff}}^5]\}$ with the peak area of the P lines with $n = 15, 17, 19$ [see Fig. 2(b)] shows good agreement, particularly as there are no adjustable parameters.

Discussion.—The plasma-physics approach used here associates the bleaching of exciton lines with the band gap renormalization due to interaction with the electron-hole plasma, akin to the Mott effect for the ground state, but studied here for Rydberg excitons with $n > 10$ at unprecedented low plasma densities. The lost oscillator strength of an exciton is transferred into the continuum. Hereby, an effective Bohr radius and an effective principal quantum number reflect the interaction with the plasma.

In Ref. [6], we performed one- and two-color pump-probe experiments, in which either only the probe scanned the exciton spectrum, or we applied an additional pump, but with the pump photon energy well below the band gap. Experimentally, this led to a similar phenomenology: bleaching of exciton absorption lines with increasing probe or pump intensity. We attributed this effect to the Rydberg blockade, where the presence of a Rydberg exciton leads to a change of the exciton absorption lines in its vicinity [6,32], while according to established models, the band gap is not shifted. However, also for excitation energies well below the band gap an electron-hole plasma is created, especially at high pump powers (see Supplemental Material [24]). Therefore, the plasma effect and the Rydberg blockade most likely always contribute simultaneously to the observations. Indeed, transferring our current understanding to the data in Figs. 3(a) and 3(d) from Ref. [6], one notes that the region of flat absorption extends towards lower energies with increasing pump power, which may be a consequence of a band gap reduction. However, by investigating excitons with low quantum numbers in the range around $n = 6$, we found clear signatures for an almost pure Rydberg blockade, see Supplemental Material [24].

Thus, we have two seemingly distinct effects that cause bleaching of exciton resonances: here, exciton lines disappear because of band gap reduction by the electron-hole plasma, leaving the exciton energies unchanged, while in the other case exciton absorption lines shift due to exciton-exciton interactions, while the band gap remains unaffected [6]. Based on the fundamental Coulomb interaction, this distinction appears artificial, raising immediate questions: (i) When exciting below the band gap, do large-sized excitons indeed leave the band gap unchanged? (ii) When exciting above the band gap, do Rydberg excitons formed by electron-hole relaxation [33] contribute to exciton bleaching? A challenge for future research is the development of a unified description comprising the effect of excitons and plasma on the exciton spectrum.

Here, we used an effective mean-field plasma description of our data. At low plasma densities, a microscopic

description of the interaction with individual charges might be feasible. The charges lead to a partial or full exciton dissociation via the Stark effect. The fully dissociated states resemble a shift of the continuum edge to lower energies with increasing excitation power, whereas the partially ionized states lose oscillator strength to the continuum, see Fig. 1. A detailed analysis of this approach is part of the ongoing research.

Conclusions.—We have studied the Rydberg exciton absorption under the influence of a driven electron-hole plasma in Cu_2O. The plasma reduces the band gap, diminishing the maximum excitable Rydberg state. High spectral resolution has allowed us to demonstrate the disappearance of an exciton when it is crossed by the band gap. These findings are intimately related to the question of the highest observable principal quantum number. Crystals contain uncompensated impurities causing a band gap renormalization. In the record $n = 25$ observations of Ref. [6], the effective band edge was shifted by 150 μeV. For observing higher n, purer samples with impurity concentrations below 0.01 cm^{-3} would be required.

[1] M. Capizzi, S. Modesti, A. Frova, J. L. Staehli, M. Guzzi, and R. A. Logan, Phys. Rev. B **29,** 2028 (1984).

[2] J. Collet, J. Phys. Chem. Solids **46,** 417 (1985).

[3] C. F. Klingshirn, *Semiconductor Optics* (Springer, Berlin, 2012), and references therein.

[4] N. F. Mott, Rev. Mod. Phys. **40,** 677 (1968).

[5] G. B. Norris and K. K. Bajaj, Phys. Rev. B **26,** 6706 (1982).

[6] T. Kazimierczuk, D. Fröhlich, S. Scheel, H. Stolz, and M. Bayer, Nature (London) **514,** 343 (2014).

[7] Because of symmetry restrictions of the involved bands in Cu_2O, the direct band-to-band transitions are dipole forbidden [8]. Taking the exciton envelope into account, the transitions to S excitons remain weak but the P excitons become dipole allowed; see also Ch. Uihlein, D. Fröhlich, and R. Kenklies, Phys. Rev. B **23,** 2731 (1981).

[8] R. J. Elliott, Phys. Rev. **108,** 1384 (1957).

[9] The Coulomb interaction does not only lead to the bound exciton states below the band gap, but also shuffles oscillator strength from higher energies towards the band gap such that the absorption becomes almost steplike above the gap, see H. Haug and S. Koch, *Quantum Theory of the Optical and Electronic Properties of Semiconductors* (Word Scientific, Singapore, 1993).

[10] T. Itoh and S. Narita, J. Phys. Soc. Jpn. **39,** 140 (1975).

[11] S. John, C. Soukoulis, M. H. Cohen, and E. N. Economou, Phys. Rev. Lett. **57,** 1777 (1986).

[12] H. J. Park and K. Natesan, Oxid. Met. **39,** 411 (1993).

[13] F. Schöne, S.-O. Krüger, P. Grünwald, H. Stolz, S. Scheel, M. Aßmann, J. Heckötter, J. Thewes, D. Fröhlich, and M. Bayer, Phys. Rev. B **93,** 075203 (2016).

[14] Indeed, at the highest applied laser powers around 10 mW, corresponding to a plasma density of 1 μm^{-3}, one finds indications for line broadening in Fig. 1, in agreement with the observations in Ref. [6]. However, only excitons up to $n = 12$ can then be observed. All higher-lying excitons disappear before any notable line broadening takes place.

[15] D. Kremp, M. Schlanges, and W.-D. Kraeft, *Quantum Statistics of Nonideal Plasmas* (Springer, Berlin, 2005).

[16] P. Grünwald, M. Aßmann, J. Heckötter, D. Fröhlich, M. Bayer, H. Stolz, and S. Scheel, Phys. Rev. Lett. **117,** 133003 (2016).

[17] The peak area is normalized by a factor 0.78×10^{-8} cm/μeV which is obtained from comparing peak area and oscillator strength at lower n that are not influenced by the plasma.

[18] R. Zimmermann, Phys. Status Solidi B **146,** 371 (1988).

[19] D. Semkat, F. Richter, D. Kremp, G. Manzke, W.-D. Kraeft, and K. Henneberger, Phys. Rev. B **80,** 155201 (2009).

[20] G. Manzke, D. Semkat, F. Richter, D. Kremp, and K. Henneberger, J. Phys. Conf. Ser. **210,** 012020 (2010).

[21] Only for much smaller T in the mK range the more general description established by Zimmermann *et al.* [18,22] would be necessary (for more recent investigations, see also Refs. [19,23]).

[22] R. Zimmermann, K. Kilimann, W. D. Kraeft, D. Kremp, and G. Röpke, Phys. Stat. Solidi B **90,** 175 (1978).

[23] G. Manzke, D. Semkat, and H. Stolz, New J. Phys. **14,** 095002 (2012).

[24] See Supplemental Material at http://link.aps.org/supplemental/10.1103/PhysRevLett.121.097401, that includes Refs. [25–28], for details on the calculations of electron and hole temperatures, the conversion from pump laser power into a plasma density, and a comparison between plasma effects and Rydberg blockade.

[25] H. Stolz, R. Schwartz, F. Kieseling, S. Som, M. Kaupsch, S. Sobkowiak, D. Semkat, N. Naka, Th. Koch, and H. Fehske, New J. Phys. **14,** 105007 (2012).

[26] R. Schwartz, N. Naka, F. Kieseling, and H. Stolz, New J. Phys. **14,** 023054 (2012).

[27] B. K. Ridley, *Quantum Processes in Semiconductors*, 5th ed. (Oxford University Press, Oxford, 2013).

[28] C. Sandfort, J. Brandt, D. Fröhlich, M. Bayer, and H. Stolz, Phys. Rev. B **78,** 045201 (2008).

[29] S. Paul and Y. K. Ho, Phys. Plasmas **16,** 063302 (2009).

[30] J. Seidel, S. Arndt, and W. D. Kraeft, Phys. Rev. E **52,** 5387 (1995).

[31] Simultaneous optimization of a_B and n results in essentially the same dependence.

[32] M. D. Lukin, M. Fleischhauer, R. Côté, L. M. Duan, D. Jaksch, J. I. Cirac, and P. Zoller, Phys. Rev. Lett. **87,** 037901 (2001).

[33] T. Kitawa, M. Takahata, and N. Naka, J. Lumin. **192,** 808 (2017).